Physics AUC, vol. 27, 10-16 (2017)

Singularity structure of the electric field near the limiter of the tokamak

Steinbrecher György, Pometescu Nicolae
Department of Physics, University of Craiova,
Str. A. I. Cuza, No.13, 200585 - Craiova, Romania

Abstract

The simulation of the Wall Touching Kink Modes (WTKM) requieres, as an intermediate numerical step, the computation of the solution of Dirichlet problems for the interior of the toroidal chamber, when a limiter is attached. In this work the singularity structure of the electric field is investigated. It is proved that at the limiter edge the electric field intensity diverges and the exact asymptotic regime is established.

1 Introduction

In the simulation of wall touching kink modes (WTKM) in the thin wall approximation, one of the problem is the efficient approximation of the solutions of the evolution equations [1]. In the case when on the tokamak wall a metallic conducting piece, for instance a limiter, is attached, one of the problem that appears in the thin wall approximation is related to the regularity of the solutions near the edge of the limiter. The possible lack of regularity means that the speed of convergence of usual finite element discretization methods is reduced. In order to highlight the singularity structure we consider a soluble model. Because the singularity is local, and the width of the limiter is small, compared to the minor radius, we neglect the curvatures of the tokamak wall. Due to the small width of the limiter we consider that the local electrostatic equilibrium in the limiter is already established. Under these assumptions, that means that higher order harmonics in the limiter are neglected, our study is reduced to the following electrostatic problem: Find the singularity structure of solution of the Poisson equation, in the infinite domain $D_3 \subset \mathbb{R}^3$, with zero Dirichlet conditions on the boundary D_3. Without loss of generality, the domain D_3 is given by

$$D_3 = \{(x, y, z)|\ \dot{z} > 0\} \backslash L_3 \tag{1}$$

where the domain $L_3 \subset \mathbb{R}^3$ (that simulate the limiter) is

$$L_3 = \{(x, y, z)|\ x = 0;\ 0 \leq z \leq 1\} \tag{2}$$

This model domain reflects the invariance of the singularity structure of the local electric field on the limiter edge when moving in the poloidal directions along the limiter. This compact symmetry in the our model appears as the invariance along the y direction. As a result, the singularity structure study can be reduced to the two dimensional case, which in turn can be reformulated in the term of finding the Green function and its harmonic conjugate, the Neumann function, for the domain D_2 in the complex plane $\mathbb{C}$, where

$$\begin{aligned} D_2 &= \{z|\ z \in \mathbb{C},\ \operatorname{Im}(z) > 0\} \backslash L_2 \\ L_2 &= \{z|\ z \in \mathbb{C},\ 0 \leq \operatorname{Im}(z) \leq 1, \quad \operatorname{Re}(z) = 0\} \end{aligned} \tag{3}$$

Because the domain D_2 has not smooth boundary, the complex potential is not necessary differentiable on the boundary of D_2 (see [3], [2]), consequently the study of the singularity structure of the boundary value problem of the first kind (Dirichlet problem) as well as the boundary value problem of the second kind (Neumann problem) is necessary for the elaboration of numerical methods for solution of more general problems like the problem treated in [1] .

In the following we will give an explicit analytic solution for the Complex Green-Neumann function (CGNf) associated to the domain D_2. Recall that the CGNf associated to a domain is a complex valued function whose real part is the Green function and the imaginary part is its harmonic conjugate, the kernel for the associated Neumann problem. In this end we use a conformal mapping that transform the domain D_2 into upper half complex plane, were the CGNf is known. By using the resulting analytic formula, we prove that in general the electric field intensity has singular behavior near limiter edge, and the final result that in the domain D_3 the electric field intensity diverges as follows

$$|\mathbf{E}(x, y, z)| = O\left(\frac{1}{(x^2 + (z-1)^2)^{1/4}}\right);\ x \to 0;\ y \to 1 \tag{4}$$

that follows from the Equations (19, 20), (see bellow).

2 Solution of the problem

2.1 The complex Green-Neumann function

We use the convention ([2], page 75, convention used also in MATHEMATICA) in defining the "principal value" branch of the complex logarithmic function $z \to \log(z)$, with branch cut in the complex plane from $z = 0$ to $z = -\infty$. This corresponds to the branch cut of the square root function in the complex plane that give, in the case when $a,\ \varepsilon > 0$ are real numbers and $z = -a^2 \pm i\varepsilon$. The branch cut conventions are the following

$$\begin{aligned} \sqrt{z} &= +i|a| + O(\varepsilon), \quad \varepsilon > 0 \\ \sqrt{z} &= -i|a| + O(\varepsilon), \quad \varepsilon < 0 \\ z &= a + i\varepsilon \end{aligned}$$

This choice of the branch cut has the advantage that we have for the complex conjugate

$$\overline{(\sqrt{z})} = \sqrt{\overline{z}}$$

By using this conventions (no branching for real values), the conformal mapping

$$z \to w = \frac{z}{\sqrt{1+z^2}}$$

maps the upper half plane $\operatorname{Im}(z) > 0$ which is cut along the imaginary axis from $z = i$ to $z = i\infty$ onto the upper half plane $\operatorname{Im}(w) > 0$ (see [2] page 272). In this case, the positive real axis $\mathrm{Im}(z) = 0$, $\mathrm{Re}(z) > 0$ is mapped in $\mathrm{Im}(w) = 0,\ 0 < \mathrm{Re}(w) < 1$, respectively the line $\mathrm{Im}(z) = 0$, $\mathrm{Re}(z) < 0$ is mapped onto line $\mathrm{Im}(w) = 0,\ -1 < \mathrm{Re}(w) < 0$. The line $\mathrm{Re}(z) = 0,\ 0 < \mathrm{Im}(z) < 1$ is mapped onto upper imaginary axis $\mathrm{Re}(w) = 0,\ \ \mathrm{Im}(w) > 0$. The subtle part is that the right side of the branch cut

$$z = iy + \varepsilon,\ y > 1,\ \ \varepsilon > 0$$

is mapped onto

$$\mathrm{Im}\, w = 0, \quad \mathrm{Re}(w) > 1$$

respectively the left side of the branch cut

$$z = iy - \varepsilon,\ y > 1,\ \ \varepsilon > 0$$

transforms in

$$\mathrm{Im}\, w = 0, \quad \mathrm{Re}(w) < -1$$

The real points $w = \pm 1$ are attained in the limit $y \to +\infty$, $z = iy \pm \varepsilon$, with $\varepsilon > 0$.

From the previous conformal mapping we generate a new map, by composing with the map $z \to z' = -1/z$. This transformation maps the upper half plane onto itself, the line $\{iy|1 < y < \infty\}$ is mapped onto $\{iy|0 \leq y < 1\}$. The resulting map (not simplified due to branch point, because in general $\sqrt{z^2} \neq z$) is

$$z \to w = \frac{-1}{z\sqrt{1 + 1/z^2}} \tag{5}$$

The transformation from Equation (5) maps the upper half plane $\mathrm{Im}(z) > 0$, which is cut along the the imaginary axis from $z = 0$ to $z = i$, onto the upper half plane $\mathrm{Im}(w) > 0$. In this case the line $\mathrm{Re}(z) = 0$, $\mathrm{Im}(z) > 1$ is transformed in the line $\mathrm{Re}(w) = 0, \mathrm{Im}(w) > 0$, the set $\mathrm{Im}(z) = 0, \mathrm{Re}(z) > 0$ onto the set $\mathrm{Im}(w) = 0, \mathrm{Re}(w) < -1$, respectively the set $\mathrm{Im}(z) = 0$, $\mathrm{Re}(z) < 0$ onto the set $\mathrm{Im}(w) = 0$, $\mathrm{Re}(w) > 1$.

By using the same convention for the branch cut, we find that the right side of the branch cut

$$z = iy + \varepsilon,\ 0 < y < 1,\ \ \varepsilon > 0$$

is mapped onto

$$\mathrm{Im}\, w = 0, \quad \mathrm{Re}(w) > 1$$

respectively the left side of the branch cut

$$z = iy - \varepsilon,\ 0 < y < 1,\ \ \varepsilon > 0$$

transforms in the set

$$\mathrm{Im}\, w = 0, \quad \mathrm{Re}(w) < -1$$

Remark 1 *A small circle of radius δ around the expected singularity*

$$z = i + \delta \exp(i\phi); \quad -\pi/2 < \phi < 3\pi/2$$

is transformed in the large loop, approximated by a half circle in the upper half plane, of radius $1/\sqrt{2\delta}$

$$w = \frac{1}{\sqrt{2\delta}} \exp\left[i\left(\phi - \pi/2\right)/2\right]\ \left[1 + O(\delta)\right] \tag{6}$$

The complex Green-Neumann function of the upper half plane is given by the Reflection Principle ([3])

$$G_w(w, w_0) = -\frac{1}{2\pi} \log \frac{|w - w_0|}{|w - \overline{w_0}|} \tag{7}$$

where $\overline{w_0}$ is the complex conjugate of w_0. The corresponding complex Green-Neumann function in the z variable is given by

$$G_z(z, z_0) = -\frac{1}{2\pi} \log \left(\frac{\frac{1}{z\sqrt{1+\left(\frac{1}{z}\right)^2}} - u_0}{\frac{1}{z\sqrt{1+\left(\frac{1}{z}\right)^2}} - \overline{u_0}} \right) \tag{8}$$

$$u_0 = \frac{1}{z_0\sqrt{1 + \left(\frac{1}{z_0}\right)^2}} \tag{9}$$

The Green function for the Poisson equation, with Dirichlet boundary condition on $\mathrm{Im}(z) = 0$, with unit charge at z_0 is given by the real part of $G_z(z, z_0)$. So the equipotential surfaces, respectively the corresponding electric field lines are given by

$$\mathrm{Re}\, G_z(z, z_0) = const \tag{10}$$

$$\mathrm{Im}\, G_z(z, z_0) = const \tag{11}$$

3 The singularity structure

We establish the following notations, concerning the position of the external charge

$$z_0 = x_0 + y_0 i$$

Then, according to Equations(8, 9) we have the following asymptotic expansion near the singular point $z_s = i$:

$$\frac{dG_z(z, z_0)}{dz} = \frac{a_{-1/2}}{\sqrt{(z-i)}} + a_0 + a_{1/2}\sqrt{(z-i)} + a_1(z-i) + \mathcal{O}((z-i)^{3/2}) \tag{12}$$

The coefficients are given by (see Equation 9),

$$a_{-1/2} = \frac{(i-1)\,\mathrm{Im}(u_0)}{2\pi};\ a_0 = \frac{\mathrm{Im}(u_0^2)}{\pi} \tag{13}$$

$$a_{1/2} = \frac{\frac{3}{8}(1+i)\,\mathrm{Im}(u_0) + \ (1-i)\,\mathrm{Im}(u_0^3)}{\pi} \tag{14}$$

$$a_1 = \frac{i\,\mathrm{Im}(u_0^2 - 2u_0^4)}{\pi} \tag{15}$$

In our interpretation $\mathrm{Re}(G_z(z, z_0))$ is the electric potential. By Cauchy-Riemann relations, the electric field is given by

$$E_x(z) = -\,\mathrm{Re}\left(\frac{dG_z(z, z_0)}{dz}\right) \tag{16}$$

$$E_y(z) = \mathrm{Im}\left(\frac{dG_z(z, z_0)}{dz}\right) \tag{17}$$

$$z = x + iy \tag{18}$$

Consequently, by using Equations(12-17) we obtain the following asymptotic expansions near the singular point $z = i + r\exp(i\phi)$:

$$
\begin{aligned}
E_x(r,\phi;z_0) &= \frac{1}{\sqrt{r}}\left[\alpha_{-1/2}\cos(\phi/2) + \beta_{-1/2}\sin(\phi/2)\right] + \alpha_0 \\
&+\sqrt{r}\left[\alpha_{1/2}\cos(\phi/2) + \ \beta_{1/2}\sin(\phi/2)\right] \\
&+r\left[\ \alpha_1\cos(\phi) + \beta_1\sin(\phi)\right] + \mathcal{O}(r^{3/2})
\end{aligned} \tag{19}
$$

where the coefficients $\alpha, \ \ \beta$ of the asymptotic expansion are given by

$$
\begin{aligned}
\alpha_{-1/2} &= \frac{\mathrm{Im}(u_0)}{2\pi} \ \ ; \ \ \beta_{-1/2} = -\frac{\mathrm{Im}(u_0)}{2\pi} \quad ; \quad \alpha_0 = -\frac{\mathrm{Im}(u_0^2)}{\pi} \\
\alpha_{1/2} &= -\frac{1}{\pi}\left[\frac{3}{8}\mathrm{Im}(u_0) + \mathrm{Im}(u_0^3)\right] \ \ ; \ \ \beta_{1/2} = \frac{1}{\pi}\left[\frac{3}{8}\mathrm{Im}(u_0) - \mathrm{Im}(u_0^3)\right] \\
\alpha_1 &= 0 \ \ ; \quad \beta_1 = \frac{1}{\pi}\mathrm{Im}(u_0^2 - 2u_0^4)
\end{aligned}
$$

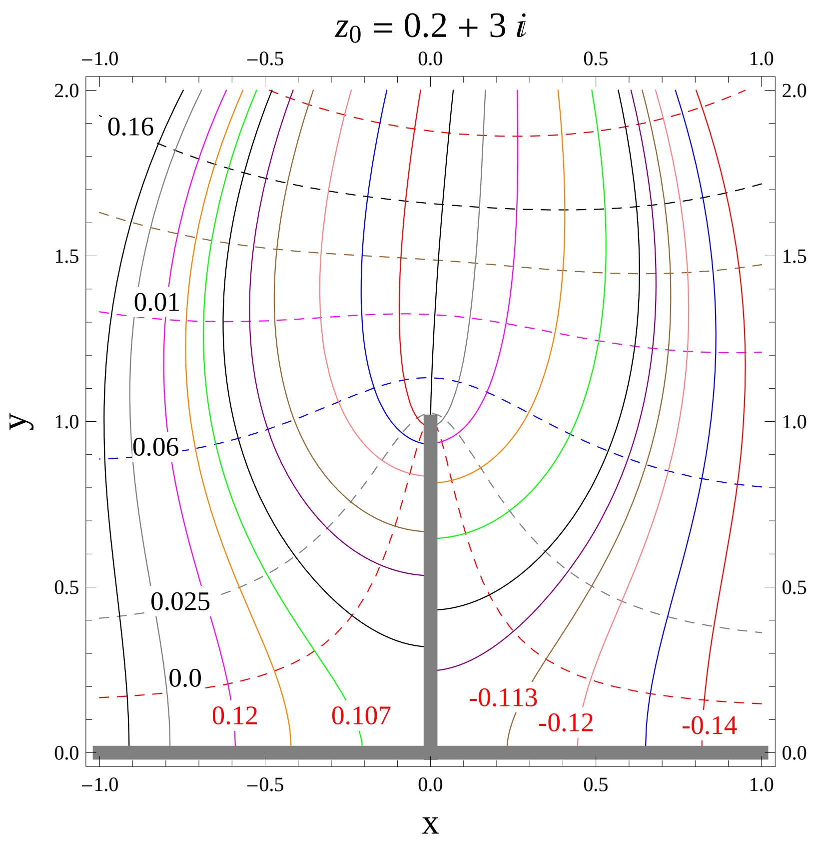

Figure 1. In the case of point charge position $z_0 = 0.2 + 3i$ are represented the echipotential curves (dashed curves) and the electric field lines (continous curves). The first ones correspond to $\mathrm{Re}\, G_z(z, z_0) = const.$ for different values of the constant (specified with black fonts). The second ones, the electric field lines (continous curves) correspond to $\mathrm{Im}\, G_z(z, z_0) = const.$ for different values of the constant (specified with red fonts). The limiter pozition is also represented.

Similar, for $E_y(z) = E_y(i + r\exp(i\phi)\ )$:

$$E_y(r,\phi;z_0) = \frac{1}{\sqrt{r}}\left[\gamma_{-1/2}\cos(\phi/2) + \delta_{-1/2}\sin(\phi/2)\right] + \gamma_0 + \sqrt{r}\left[\gamma_{1/2}\cos(\phi/2) + \delta_{1/2}\sin(\phi/2)\right] + r\left[\gamma_1\cos(\phi) + \delta_1\sin(\phi)\right] + \mathcal{O}(r^{3/2}) \tag{20}$$

where the coefficients γ, δ of the asymptotic expansions are given by

$$\begin{aligned}
\gamma_{-1/2} &= \frac{1}{2\pi}\,\mathrm{Im}(u_0) \quad , \quad \delta_{-1/2} = \frac{1}{2\pi}\,\mathrm{Im}(u_0) \quad ; \quad \gamma_0 = 0 \\
\gamma_{1/2} &= \frac{1}{\pi}\left[\frac{3}{8}\,\mathrm{Im}(u_0) - \mathrm{Im}(u_0^3)\right] \quad ; \quad \delta_{1/2} = \frac{1}{\pi}\left[\frac{3}{8}\,\mathrm{Im}(u_0) + \mathrm{Im}(u_0^3)\right] \\
\gamma_1 &= \frac{1}{\pi}\,\mathrm{Im}(u_0^2 - 2u_0^4) \quad ; \quad \delta_1 = 0
\end{aligned}$$

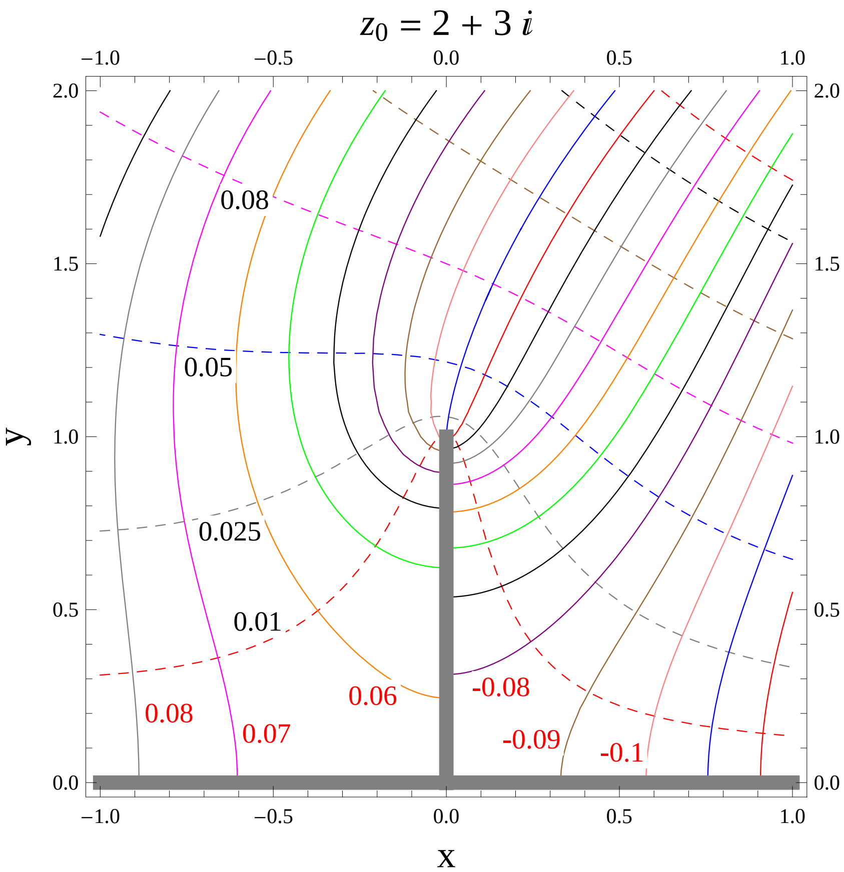

Figure 2. The point charge position is given by $z_0 = 2 + 3i$. The echipotential curves (dashed curves) and the electric field lines (continous curves) are represented. The first ones correspond to $\mathrm{Re}\,G_z(z,z_0) = const.$ for different values of the constant (specified with black fonts). The second ones, the electric field lines (continous curves) correspond to $\mathrm{Im}\,G_z(z,z_0) = const.$ for different values of the constant (specified with red fonts).

The singularity structure is visible in the Figure 1, 2, where the equipotential curves and the electric field lines in the neighborhood of the limiter are presented. The electric field is the result of the "two dimensional point charge" (in fact infinite thin wire, perpendicular to the plane) and the charge induced in the metallic structure : the tokamak wall, represented (locally) by the Ox axis, and the limiter, the line from the coordinate origin to the point $(0, 1)$.

4 Conclusions

We proved that at the limiter edge the electric field intensity induced on the tokamak metallic wall by unbalanced spatial charge in plasma, in the thin wall approximation, is divergent. It diverges as $1/\sqrt{d}$ where d is the distance from the given point to the limiter edge. It follows that in the numerical simulation it is useful to use of finite element methods that include test functions that reproduces the singularity structure in the domains that contains the points close to the limiter edge.

Acknowledgement

This work has been carried out within the framework of the EUROfusion Consortium as a complementary project and has been received funding from the Romanian National Education Minister / Institute of Atomic Physics under contract _1EU-2/2//01.07.2016. The collaboration with the Calin Vlad Atanasiu is acknowledged.

References

[1] L. E. Zakharov, C. V. Atanasiu, K. Lackner, M. Hoelzl, E. Strumberger, Electromagnetic thin wall model for simulation of plasma wall touching kink and vertical modes J. Plasma Phys. **81**, 515810610 .

[2] Z. Nehari, Conformal mapping, Dover Books in Advanced Mathematics, Dover Publications, New York (1952)

[3] N.Papamichael, N. Stylianopoulos, Numerical Conformal Mapping, Domain Decomposition and Mapping the Quadrilaterals, World Scientific, (2009).